

Article

Mathematical Modeling and Performance Analysis of a New Hybrid Solar Dryer of Lemon Slices for Controlling Drying Temperature

Wengang Hao ¹, Shuonan Liu ¹, Baoqi Mi ¹ and Yanhua Lai ^{1,2,*}

¹ School of Energy and Power Engineering, Shandong University, Jinan 250061, China; haowengangDL@163.com (W.H.); liusnnd@163.com (S.L.); sduzmbq@163.com (B.M.)

² Suzhou Institute, Shandong University, Suzhou 215028, China

* Correspondence: laiyh@sdu.edu.cn or sdu2019hvac@163.com

Received: 9 December 2019; Accepted: 9 January 2020; Published: 10 January 2020



Abstract: A new hybrid solar dryer was designed and constructed in this study, which consisted of a flat-plate solar collector with dual-function (DF-FPSC), drying chamber with glass, fan etc. The DF-FPSC was firstly applied in drying agricultural products. The innovative application of hybrid solar dryer can control the drying chamber air temperature within a suitable range by different operation strategies. Drying experiments for lemon slices in the hybrid solar dryer were conducted by comparing open sun drying (OSD). Eight mathematical models of drying characteristics were employed to select the most suitable model for describing the drying curves of lemon slices. Furthermore, energy, exergy economic and environment (4E) analysis were also adopted to analyze the drying process of lemon slices. The results show that under the same experimental condition, the drying capability of the hybrid solar dryer was stronger than that of OSD. Meanwhile, it was found that the Two term and Wang and Singh models were the most suitable for fitting the lemon slices' drying characteristics inside the hybrid solar dryer. The drying chamber air temperature can be controlled under about 60 °C during the process of lemon slices' drying. The experimental results show the feasibility and validity of the proposed hybrid solar dryer.

Keywords: mathematical modeling; hybrid solar dryer; solar collector; lemon slices; performance analysis

1. Introduction

Due to the energy crisis and environmental pollution issues, many governments are working on developing green energy to alleviate these problems. In the process of drying, it is an effective way for improving the economic efficiency of drying to reduce the energy consumption of drying systems. Drying system energy consumption is mainly affected by the dried product and energy efficiency of the drying system [1]. Hot air convection drying using a traditional energy source is not a sustainable way of drying due to environmental pollution, high investment and operating costs [2]. Solar drying has the advantages of being a renewable, free, and abundant energy source, meanwhile, the low-temperature utilization of solar energy just matches the suitable material drying temperature [3]. However, the practical application of solar drying generally needs to be supplemented by other forms of energy due to the influence of solar energy instability, periodic change, low heat collection efficiency, and so on [4–6]. Therefore, numerous research works concerning solar drying have been conducted over the past few decades.

Solar drying can be divided into four groups: open sun drying, direct solar drying, indirect solar drying and hybrid solar drying [7]. Many researchers have studied the design types of a solar

dryer. Solar thermal components are the key to distinguishing different solar drying systems. Hybrid photovoltaic-thermal (PV/T), solar air collector types, greenhouses, etc. have been adopted in previous literature reviews. Banout et al. [8] designed a new model of double-pass solar drier and tested it under tropical conditions in central Vietnam. Tiwari et al. [9] proposed a hybrid pPV/T greenhouse solar dryer under mixed mode. Elkhadraoui, A. et al. [10] investigated a forced convection solar greenhouse dryer; this dryer consisted of a solar air collector and chapel-shaped greenhouse. Kabeel and Abdelgaied [11] investigated a new solar dryer with rotary desiccant wheel. In addition, other different types of solar drying system have also been designed and investigated such as Janjai, S. [12], Aktaş, Mustafa [13], Sonthikun, Sonthawi [14] et al.

After the solar drying system is determined, the characteristics and operational analysis of the drying system need to be studied. On the one hand, drying characteristics of various agricultural products were also widely reported in the different solar drying systems. Can [15] investigated the drying kinetics of pumpkinseeds. Gulcimen et al. [16] performed an experimental and theoretical study on the drying of sweet basil with solar air collectors, and the drying kinetics mathematical modeling of sweet basil was found. Ali et al. [17] studied the drying kinetics of sewage sludge at different drying temperatures under the same air flow rate condition, the influencing factors on the product drying process were investigated, and the best suitable mathematical model was found. Moreover, rubber sheet [18], red pepper [19], seedless grapes [20], thymus and mint [21] were also studied to select the best suitable drying characteristics mathematical model.

On the other hand, the operational performance and evaluation of the drying materials of the solar drying system need to be analyzed and optimized. Energy analysis can provide the quantity of energy required and can determine the quality of energy and analyse irreversible causes and directions of processes in thermodynamics [3]. Rabha et al. [22] proposed and studied a solar tunnel dryer by energy and exergy analysis; the average overall thermal efficiency of solar air collector ranged from 22.95% to 23.30%. Fudholi et al. [23] studied the red seaweed drying process using energy and exergy analysis. Akbulut and Durmuş [24] investigated the mulberry drying process with energy and exergy analysis, and the maximum value of exergy loss was 10.82 W, the maximum value of energy utilization ratio was 55.2%, and the exergetic efficiency increased with the increase of drying air mass flow rate. Midilli and Kucuk [25] studied a solar drying cabinet for drying pistachios with energy and exergy analysis. In addition, photovoltaic/thermal integrated with a solar greenhouse were performed by Nayak and Tiwari [26] using the energy and exergy method. Aktaş et al. [13] presented solar heat-recovery solar drying, with solar air collector efficiency of 50.6% being obtained. Janjai et al. [12] investigated a PV-ventilated solar greenhouse dryer by employing qualities of dried product and economic evaluation. Sarhaddi et al. [27] studied the exergetic performance of a PV/T air collector. Environmental analysis and mathematical modeling of modified greenhouse dryer were conducted by Prakash and Kumar [28].

From the above literature review, the DF-FPSC has not yet been applied in drying agricultural products. Lemon is a more popular fruits for most people being rich in nutrients such as vitamin C, carbohydrate, calcium and minerals. There are few studies on lemon slices' solar drying in the current research literature, among which Chen et al. [29] proposed and built the closed-type dryer and Wang et al. [30] presented the far-infrared assisted vacuum dryer for drying lemon slices. In addition, energy, exergy, economic and environmental (4E) comprehensive evaluations of solar drying have not been studied so far.

Thus, the goals of this paper are to propose and study a new hybrid solar dryer with a flat-plate solar collector with dual-function (DF-FPSC) for drying lemon slices and to develop a most suitable drying characteristics mathematical model for lemon slices. The advantage of this study is to control the suitable air drying temperature for drying lemon slices. Furthermore, energy, exergy economic and environmental analysis of the dryer operation process were also carried out.

2. Materials and Methods

2.1. Description of System

The new hybrid solar dryer with DF-FPSC was designed and established by the author of this paper at Jinan city, located at Shandong province, China. According to the previous study results [4,31], the maximum hot air drying temperature for lemon slices should not exceed 60 °C. Therefore, the maximum temperature of the drying chamber inside air was set as 60 °C in this study. The schematic diagram of the working principle of the hybrid solar dryer is shown in Figure 1. When the drying temperature is lower than 60 °C, the outdoor air is heated by the collector absorbing energy, and then sent to the cabinet, as shown in Figure 1a. When drying temperature is higher than 60 °C, the collector absorbing energy is divided into two parts, one for drying lemon slices and the other for storing energy in the water tank as shown in Figure 1b. In the operation process of hybrid solar dryer, the operation modes of DF-FPSC include air cycle and air and water cycle simultaneous. When drying temperature is higher than 60 °C, the air and water cycle of the DF-FPSC were simultaneously opened by water pump and fan.

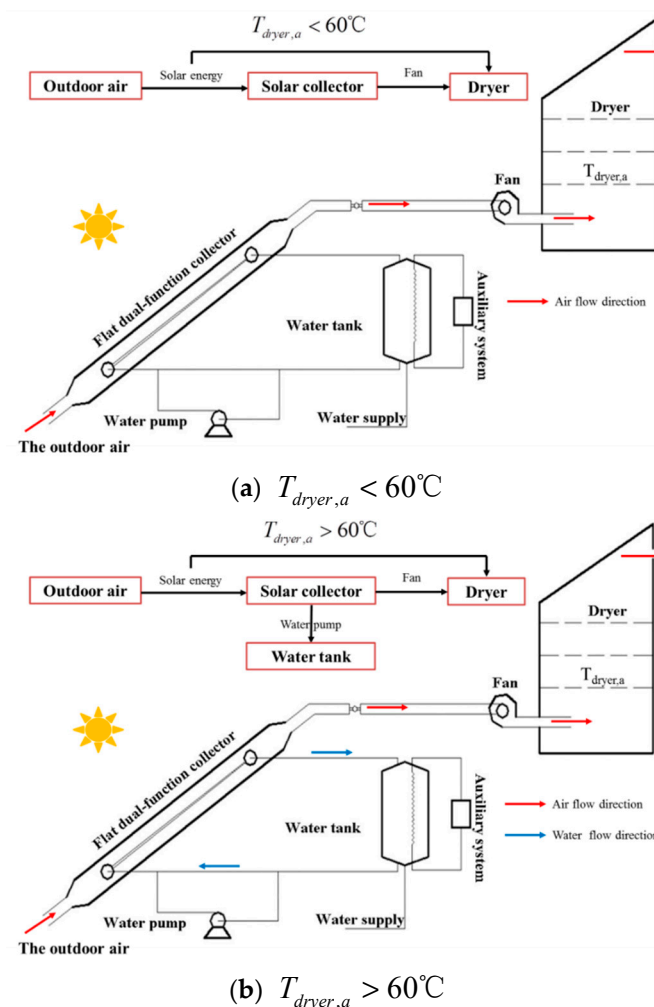


Figure 1. The schematic diagram of hybrid solar dryer operation.

The hybrid solar dryer includes DF-FPSC, water pump, fan, water tank, auxiliary electric heating and drying chamber etc. The photograph of the hybrid solar dryer is shown in Figure 2. The system composition characteristic parameters are listed in Table 1. The other detailed descriptions of the system can be referenced to [32].

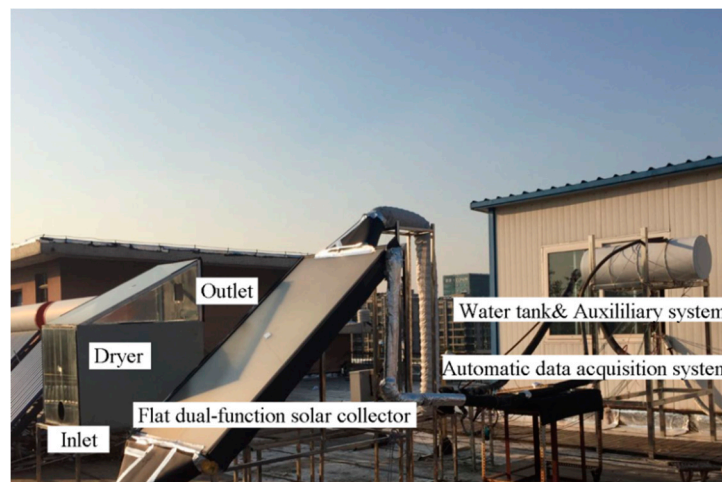


Figure 2. Photograph of hybrid solar dryer.

Table 1. The system composition characteristic parameters.

Component Name	Function	Characteristic Parameters
Flat-plate solar collector with dual-function (DF-FPSC)	Converting solar energy into hot air or hot water	Dual air and water channel. Size: 2 m × 1 m × 0.15 m (L × W × H). Total volume: 0.77 m ³ . Inclination: of 26.7°
Cabinet	Drying sample material	
Fan	Driving air flow	Fan power of 80 W
Water tank	Storing hot water	Water tank bulk of 120 mL
Water pump	Driving water flow	Pump power of 200 W
Auxiliary system	Providing extra heating energy	Electric heating power of 800 W
Tray	Placing the drying material	Size: 0.6 m × 0.3 m (L × W).

The schematic diagram of the drying chamber is shown in Figure 3. Material trays with the wire mesh of evenly spaced pores are placed in the drying chamber. In addition, the air outlet of the DF-FPSC is connected to the drying chamber air inlet through the ventilation pipe with a diameter of 110 mm. The water channel of the DF-FPSC is connected to the water tank through the water pipe with a diameter of 32 mm. The hybrid solar dryer operation is controlled by temperature control device according to the air temperature in the drying chamber.

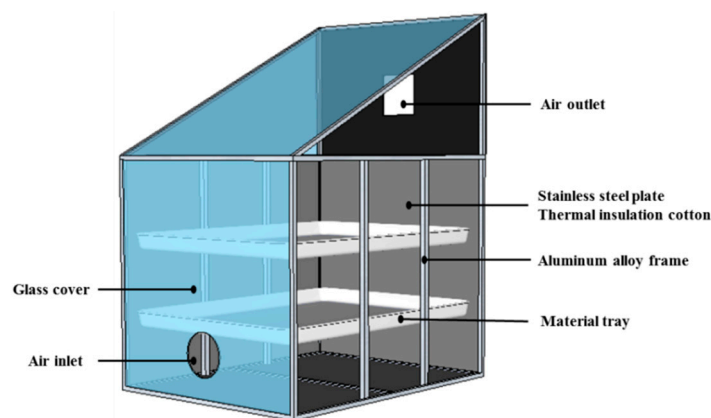


Figure 3. Schematic diagram of drying chamber.

2.2. Sample Preparation

Fresh lemons were purchased from the RT-mart (at Jinan city, Shandong province). For testing the moisture content of lemon, the lemon slices were placed in a drying oven with the temperature of 105 °C for 24 h [33]. The average initial moisture content (wet basis) of the fresh lemons was tested as 82.8%. In order to reduce errors caused by drying raw materials, the lemons used in this experiment were selected according to the same species and purchase batches. The lemons chosen were almost the same size. The fresh lemons without pre-treatment were sliced with the similar size (diameter: 5 ± 0.2 cm, thickness: 0.3 ± 0.1 cm). For each of the tests, the sample weights of an experimental group and a contrast group were selected from 300~400 g for studying drying characteristics. In addition, the mass of drying fresh lemons was selected at about 4 kg for studying the operational performance of the hybrid solar dryer.

2.3. Experimental Procedure

In order to meet the objective of this research, the drying experiment was carried out twice. One set of experiments was conducted to study the drying characteristics of lemon slices; the other set of experiments was carried out to study the operational performance of hybrid solar dryer. In the drying characteristics of lemon slices experiment, two drying methods for lemon slices were employed; one was OSD, the other was the new hybrid solar dryer. The drying process was terminated until the change of samples quality is less than ± 1 g for studying drying characteristics and ± 10 g for studying the operation performance of hybrid solar dryer. Lemon slice drying experiments were carried out in June 2018 from 08:30 to 18:00. The measurement variables included air temperature (inlet and outlet of collector, inlet and outlet of drying chamber, ambient and drying chamber inside), relative humidity (inlet and outlet of drying chamber, ambient and drying chamber inside), water temperature (inlet and outlet of collector), solar radiation intensity, electrical consumption of fan and pump, mass of drying lemon slices, mass rate of drying air and water. The schematic diagram of the experimental test system is shown in Figure 4. The test instruments characteristics were listed in Table 2. The experimental data are recorded automatically every 10 min, and the data collection was connected to the computer.

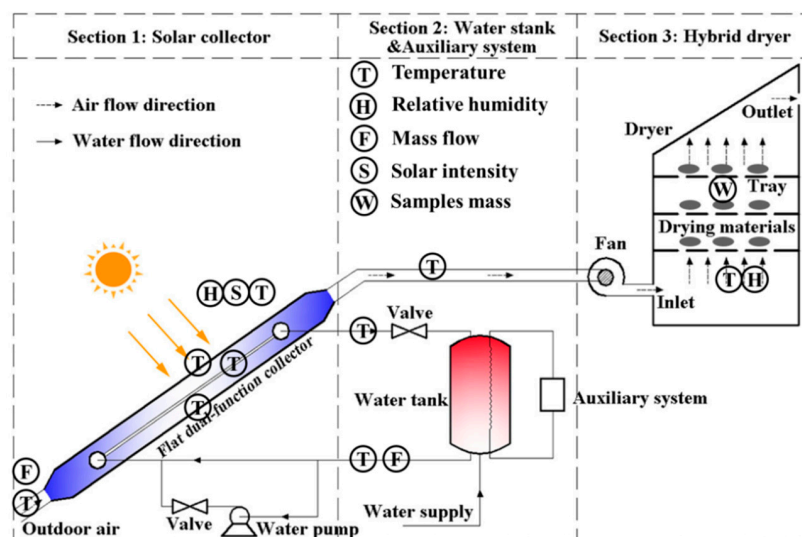


Figure 4. The schematic diagram of the experimental test system.

2.4. Uncertainty Analysis

In general, the R value of experimental results uncertainty may be calculated by a set of independent measurements, namely x_1, x_2, \dots, x_n . The uncertainty of the experimental results R can be calculated as follows [22]:

$$w_R = \left[\left(\frac{\partial R}{\partial x_1} w_1 \right)^2 + \left(\frac{\partial R}{\partial x_2} w_2 \right)^2 + \dots + \left(\frac{\partial R}{\partial x_n} w_n \right)^2 \right]^{\frac{1}{2}} \quad (1)$$

The independent parameters measured in this study were solar radiation intensity, ambient temperature and relative humidity, samples' mass, temperature (drying air temperature and relative humidity, air outlet temperature of collector, water inlet and outlet temperature of collector), air and water mass flow rate of the collector. The dependent parameters measured include solar collector efficiency, thermal efficiency and exergy efficiency. Uncertainties in different measurement variables of the experiments are listed in Table 3.

Table 2. Characteristics of the test instrument.

Instruments Name	Measuring Parameters	Range	Accuracy
TBQ-2 Pyranometer	Solar radiation intensity	0~2000 W/m ²	2%
T type thermocouple	temperature	-200~350 °C	±0.5 °C
Temperature and humidity tester	Air relative humidity	0~100%	3%
Air flow meter	Mass flow rate of air	0~500 m ³ /h	1%
Water flow meter	Mass flow rate of water	0~15 m ³ /h	1%
Electronic balance	Samples mass	0~10 kg	±0.1 g
Clamp meter Testo 770-3	Power of fan and pump	Alternating/direct current (0~600 A) Alternating/direct voltage (0~600 V)	Alternating/direct current (± 2%) Alternating/direct voltage (± 1%)

Table 3. Different experimental variables' uncertainty values.

Name	Value
Solar radiation	2.8 W/m ²
Temperature	1 °C
Mass flow rate (air and water)	1.4 m ³ /h
Power	0.04 W
Air relative humidity	4.24%
Sample mass	0.52 kg
Thermal efficiency of collector	3.44%
Drying system thermal efficiency	2%
Drying system exergy efficiency	2.43%

3. Performance Analysis

3.1. Drying Analysis

The moisture content of the lemon slices at the initial time is determined on a dry basis (d.b) as:

$$M_{d,0} = \frac{W_0 - W_d}{W_d} \quad (2)$$

The moisture content of the lemon slices at initial time is determined on a wet basis (w.b) as:

$$M_{w,0} = \frac{W_0 - W_d}{W_0} \quad (3)$$

The drying rate of lemon slices during drying experiments can be expressed using the following equations:

$$DR = \frac{M_{t+dt} - M_t}{dt} \quad (4)$$

The quantity of water can be calculated as:

$$W_f = \frac{(M_0 - M_f)}{(100 - M_f)} \times W_0 \quad (5)$$

The instantaneous moisture content can be defined as:

$$M_t = \left[\frac{(M_0 + 1)W_t}{W_0} - 1 \right] \quad (6)$$

The relation between dry basis and wet basis can be expressed as:

$$M_w = 1 - \left(\frac{1}{M_d + 1} \right) \quad (7)$$

The moisture ratio MR is defined as:

$$MR = \frac{M_t - M_e}{M_0 - M_e} \quad (8)$$

Due to M_e Far less than M_0 , the above equation can be simplified as:

$$MR = \frac{M_t}{M_0} \quad (9)$$

Drying mathematical models were used to select the most suitable model for describing the drying curves of lemon slices during the drying process, as given in Table 4. The regression analysis was performed by using the Statistical Package for Social Scientists (SPSS) 17 software package. The coefficient of determination R^2 and root mean square error (RMSE) was also applied to select the most suitable models.

The above statistical parameters can be calculated using the following equations:

$$R^2 = \frac{\sum_{i=1}^N (MR_i - MR_{pre,i}) \cdot \sum_{i=1}^N (MR_i - MR_{exp,i})}{\sqrt{\left[\sum_{i=1}^N (MR_i - MR_{pre,i})^2 \right] \left[\sum_{i=1}^N (MR_i - MR_{exp,i})^2 \right]}} \quad (10)$$

$$RMSE = \left[\frac{1}{N} \sum_{i=1}^N (MR_{exp,i} - MR_{pre,i})^2 \right]^{\frac{1}{2}} \quad (11)$$

Table 4. Drying curve models for lemon slices.

Number	Model Name	Model Equation	Ref.
1	Newton	$MR = \exp(-k \times t)$	[34]
2	Page	$MR = \exp(-k \times t^n)$	[35]
3	Henderson and pabis	$MR = \alpha \times \exp(-k \times t)$	[36]
4	Logarithmic	$MR = \alpha \times \exp(-k \times t) + c$	[37]
5	Two term	$MR = \alpha \times \exp(-k_0 \times t) + b \times \exp(-k_1 \times t)$	[38]
6	Wang and Singh	$MR = 1 + \alpha \times t + b \times t^2$	[39]
7	Modified Page	$MR = \exp(-(kt)^n)$	[40]
8	Thompson	$t = \alpha \times \ln(MR) + b \times (\ln(MR))^2$	[41]

3.2. Energy Analysis

The energy analyses of the hybrid solar dryer were carried out by the conservation of mass and energy. In the process of lemon slices' drying, the energy inflows of the hybrid solar dryer include solar energy and electric energy used by the fan and pump, the energy outflows of the hybrid solar dryer include heat losses of different locations (solar collector, connection duct, drying chamber et al.) and the drying air of the drying chamber outlet.

The general mass conservation equation of drying air can be expressed as follows:

$$\sum \dot{m}_{a,in} = \sum \dot{m}_{a,out} \quad (12)$$

The general mass conservation equation of moisture can be calculated as follows:

$$\sum (\dot{m}_{a,in}w_{in} + \dot{m}_{mp}) = \sum \dot{m}_{a,out}w_{out} \quad (13)$$

The general equation of energy conservation can be expressed as follows:

$$Q - W = \sum m_{a,out} \left(h_{out} + \frac{V_{out}^2}{2} \right) - \sum m_{a,in} \left(h_{in} + \frac{V_{in}^2}{2} \right) \quad (14)$$

During the energy analyses, the following assumptions can be made:

- The drying air flow was assumed to be steady [25].
- The hybrid solar dryer was the same horizontal line.
- The kinetic energies of the hybrid solar dryer can be neglected [22].

Therefore, the energy conservation of the lemon slices' drying process can be determined as follows based on the above assumptions and equations:

$$Q - W = m_a(h_{out} - h_{in}) \quad (15)$$

The relative humidity of drying air can be calculated as follows:

$$\phi = \frac{wP}{(0.622 + w)P_{sat@T}} \quad (16)$$

The collector efficiency was calculated by:

$$\eta = \frac{Q_u}{\alpha\tau IA_c} \quad (17)$$

The enthalpy of drying air can be expressed:

$$h = C_{p,a}T_a + wh_{sat@T} \quad (18)$$

The useful heat gained of collector can be calculated by:

$$Q_u = \begin{cases} m_a C_{p,a} (T_{ou,a} - T_{in,a}) & \text{only air cycle} \\ m_w C_{p,w} (T_{ou,w} - T_{in,w}) & \text{only water cycle} \\ m_a C_{p,a} (T_{ou,a} - T_{in,a}) + m_w C_{p,w} (T_{ou,w} - T_{in,w}) & \text{air and water cycle simultaneously} \end{cases} \quad (19)$$

The specify energy consumption (SEC) of system can be defined as follows:

$$SEC = \frac{Q_u + E_{fan} + E_p}{m_w} \quad (20)$$

The mass of water removed can be estimated by:

$$m_w = \frac{m_p(m_i - m_f)}{100 - m_f} \quad (21)$$

The system drying efficiency can be calculated as follows:

$$\eta = \frac{m_w h_{ev}}{IA_c + E_f + E_p} \quad (22)$$

The theoretical thermal efficiency can be calculated by:

$$\eta_{th} = \frac{T_{dc} - T_{dc.out}}{T_{dc} - T_{amb}} \quad (23)$$

3.3. Exergy Analysis

In general, the exergy losses of the drying chamber include the exergy loss of the drying chamber wall heat dissipation, the exergy loss of drying air, and the exergy loss of the product. The following assumptions were made:

- The flow of drying air can be assumed to be steady.
- The exergy loss of the product was neglected due to the type of chamber.
- The variation of drying air moisture content was neglected [22].
- The change of pressure in the inlet and outlet of drying chamber was neglected.

Therefore, the flow exergy of steady flow stream of drying chamber can be given by:

$$Ex = m_a C_{p,a} \left[(T - T_r) - T_r \ln \left(\frac{T}{T_r} \right) \right] \quad (24)$$

The exergy of drying chamber inlet can be given by:

$$Ex_{in} = m_a C_{p,a} \left[(T_{dc} - T_r) - T_r \ln \left(\frac{T_{dc}}{T_r} \right) \right] \quad (25)$$

The exergy of drying chamber outlet can be given by:

$$Ex_{out} = m_a C_{p,a} \left[(T_{out} - T_r) - T_r \ln \left(\frac{T_{out}}{T_r} \right) \right] \quad (26)$$

Thus, the exergy losses of the drying chamber can be determined by:

$$\sum Ex_{loss} = \sum Ex_{in} - \sum Ex_{out} \quad (27)$$

The exergetic efficiency of drying chamber can be written as:

$$\eta_{Ex} = \frac{Ex_{out}}{Ex_{in}} = 1 - \frac{Ex_{loss}}{Ex_{in}} \quad (28)$$

The improvement potential (IP) of the novel hybrid solar dryer can be given as:

$$IP = (1 - \eta_{Ex}) Ex_{loss} \quad (29)$$

3.4. Economic Analysis

The capital costs of the hybrid solar dryer include material cost and construction cost, which can be obtained from a local market. It can be calculated by:

$$C_t = C_m + C_c \quad (30)$$

The annual cost calculation method was proposed by Audsley and Wheeler [42] and can be expressed by:

$$C_a = \left[C_t + \sum_{i=1}^N (C_{\text{maint}} + C_{\text{optera}}) Z^i \right] \left(\frac{Z-1}{Z(Z^N-1)} \right) \quad (31)$$

where

$$Z = \frac{100 + i_m}{100 + i_f} \quad (32)$$

The operating cost of the hybrid solar dryer include only the electricity consumption cost (fan and pump), and it can be calculated by:

$$C_{\text{optera}} = E_{\text{fan}} \cdot t_{\text{fan}} + E_p \cdot t_p \quad (33)$$

The maintenance cost of the hybrid solar dryer was equal to 1% of the capital cost. The cost per unit of drying materials can be calculated by:

$$F = \frac{C_a}{M_d} \quad (34)$$

The payback period can be calculated by:

$$PBP = \frac{C_t}{M_d P_d - M_f P_f - M_d F} \quad (35)$$

3.5. Environmental Analysis

In the drying process, the CO₂ reductions per batch based on results of this experiment can be calculated as follows [43]:

$$R_{\text{CO}_2} = \frac{\psi_{\text{CO}_2} \cdot Q_{u,\text{overall}}}{1000} \quad (36)$$

The CO₂ emission of system per batch drying products can be obtained as follows:

$$EM_{\text{CO}_2} = (E_{\text{fan}} + E_p) \cdot \psi_{\text{CO}_2} \quad (37)$$

The revenue of CO₂ abatement was calculated by:

$$Y_{\text{CO}_2} = CP_{\text{CO}_2} \cdot (R_{\text{CO}_2} - EM_{\text{CO}_2}) \quad (38)$$

4. Results and Discussion

4.1. Drying Characteristics

The set of experimental data for studying the drying characteristics of lemon slices were performed on 7 and 8 June 2018. The change of solar radiation intensity was shown in Figure 5. The maximum values of solar radiation intensity at two days were 424 W/m² and 438 W/m², respectively, and the average values of solar radiation intensity were 257.36 W/m² and 218.33 W/m², respectively. The maximum values of solar radiation intensity at two days occurred at 12:30 and 11:40, respectively. The solar radiation intensity increased gradually to the maximum value and then decreased during the period of the drying experiment.

The change of air temperature and relative humidity is shown in Figure 6. The range of ambient temperature was 28~38.5 °C. Meanwhile, the range of temperature inside drying chamber was 28.5~60.2 °C. The average temperature of drying cabinet was about 44 °C. The range of ambient

environment relative humidity was 22.4%~44.5%. Meanwhile, the relative humidity range inside drying chamber was 11.7%~38.1%. The maximum temperature of drying chamber was almost equal to the experiments set value. These results show that the operation parameters can meet design requirement in terms of controlling the drying temperature of the drying chamber.

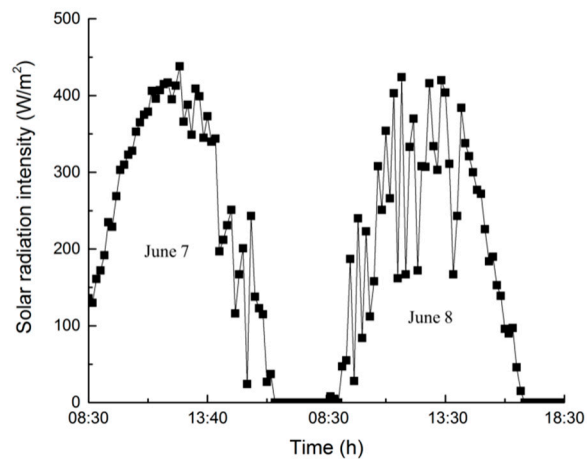


Figure 5. The change of solar radiation intensity.

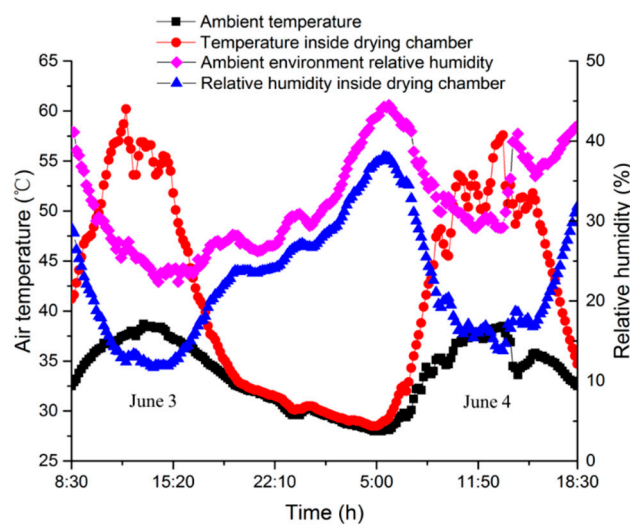


Figure 6. The change of air temperature and relative humidity.

4.1.1. Drying Kinetics

The change of lemon slices' moisture content is shown in Figure 7. The lemon slices moisture content of OSD was 0.455 g g^{-1} higher than that of hybrid solar dryer at the end of first day, and lemon slices' moisture content of OSD was 0.598 g g^{-1} higher than that of hybrid solar dryer at the end of second day of drying. The lemon slices moisture content of OSD and hybrid solar dryer was 0.905 g g^{-1} and 0.307 g g^{-1} respectively at the end of drying. These results indicate that the drying capacity of the hybrid solar dryer is higher than that of OSD under the same conditions. Furthermore, according to Figure 6, drying temperature has an important influence on the different solar drying curves of lemon slices. It is consistent with the problems revealed by the factors influencing the effective diffusion rate in material drying [10,17,44].

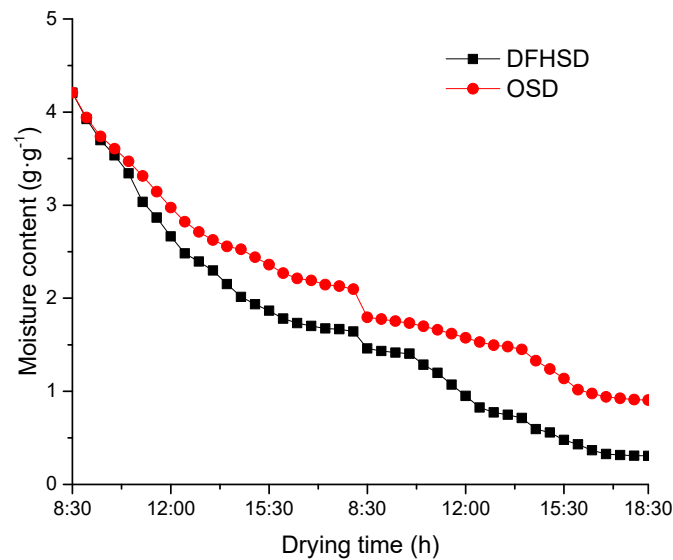


Figure 7. The change of lemon slices moisture content.

Figure 8 represented the change of moisture ratio for lemon slices. The moisture ratio ranged from 1 to final moisture ratio of about 0.073 inside hybrid solar dryer. Meanwhile, the moisture ratio ranged from 1 to the final moisture ratio of about 0.215 under the OSD operation mode. These results again indicate that the hybrid solar dryer drying capacity was higher than that of OSD under the same conditions.

In addition, the decrease in the rate of the moisture ratio was faster at the beginning of the drying experiment and later decreased, as shown in Figure 8. This is because the lemon slices' surface water evaporated during the initial drying process, and the water content of lemon slices diffuses from inside to the surface of drying materials. These results were also verified by previous research [45,46].

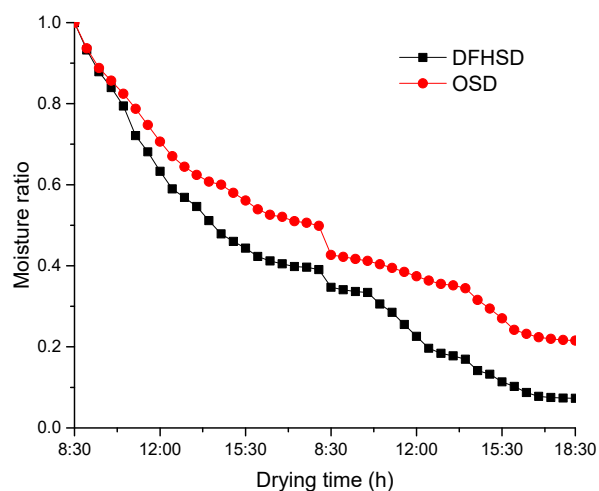


Figure 8. The change of moisture ratio for lemon slices' drying.

4.1.2. Drying Rates Curves

Figure 9 shows the change of lemon slices' drying rate of the typical experiments. The drying rate of lemon slices at the first day was higher than that on the second day. The average drying rate of lemon slices for the hybrid solar dryer and OSD was $0.262 \text{ g g}^{-1} \text{ s}^{-1}$ and $0.229 \text{ g g}^{-1} \text{ s}^{-1}$, respectively, on the first day. The average drying rate of lemon slices for the hybrid solar dryer and OSD was $0.109 \text{ g g}^{-1} \text{ s}^{-1}$

and $0.085 \text{ g g}^{-1} \text{ s}^{-1}$, respectively, on the second day. The average drying rate of lemon slices for hybrid solar dryer was faster than OSD due to the high temperature of drying air. Combined with the results of Figure 6, these results show that the drying rate of lemon slices is affected significantly by the drying air temperature. The drying capacity of the hybrid solar dryer was higher than OSD.

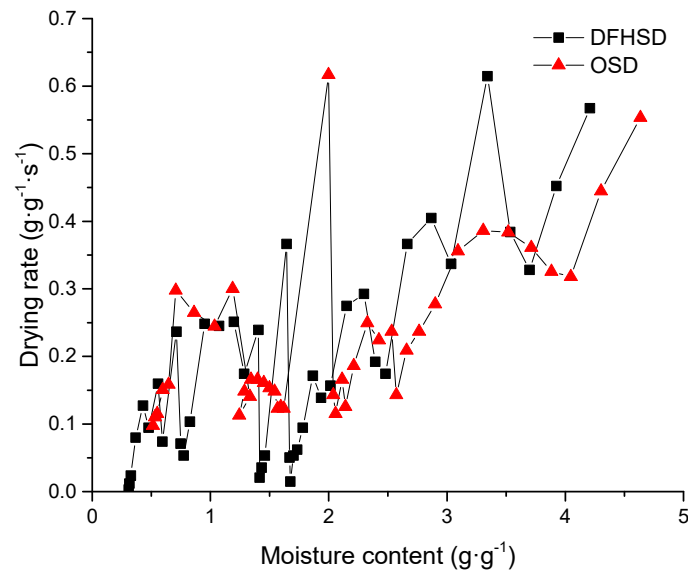


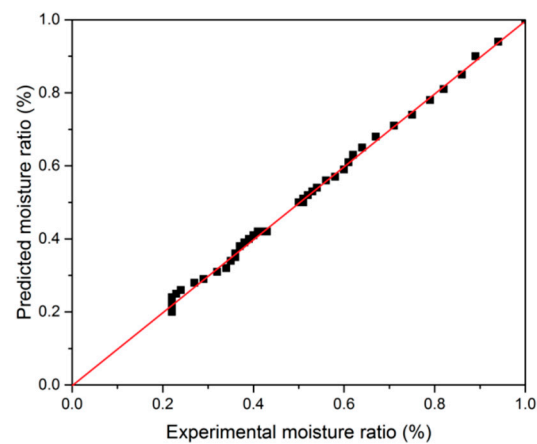
Figure 9. The change of drying rate for lemon slices’ drying.

4.1.3. Fitting of Drying Model

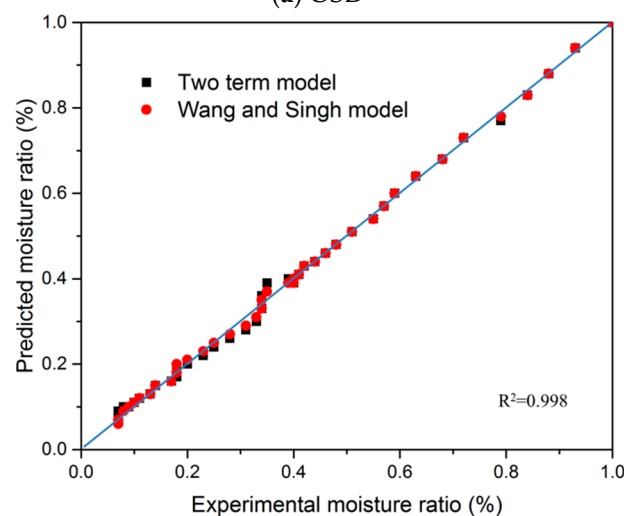
The highest value of R^2 and the lowest value of root mean squared error (RMSE) are used to select the drying characteristics mathematical model as shown in Table 5. It can be concluded that Two term and Wang and Singh were the best model for fitting the lemon slices drying with R^2 value of 0.998 and RMSE value of 0.001 for the hybrid solar dryer. Two term was the best model with R^2 value of 0.998 and RMSE value of 0.001 for OSD. The relationship between predicted and experimental values for lemon slices’ drying are shown in Figure 10. The predicted values can be fitted into a line with the slope of 1. Therefore, the Two term model and Wang and Singh model are the most suitable to describe the drying characteristics of lemon slices under hybrid solar dryer. Two term model is the most suitable to describe the drying characteristics of lemon slices under OSD.

Table 5. Non-linear regression analyses for lemon slices’ drying.

Name of Model	Hybrid Solar Dryer			Open Sun Drying (OSD)		
	Constant Coefficients	R^2	RMSE	Constant Coefficients	R^2	RMSE
Newton	$k = 0.116$	0.973	0.0617	$k = 0.083$	0.956	0.0316
Page	$k = 0.156 \ n = 0.834$	0.989	0.0742	$k = 0.128 \ n = 0.767$	0.992	0.0138
Henderson and pabis	$a = 0.965 \ k = 0.109$	0.979	0.0276	$a = 0.953 \ k = 0.075$	0.974	0.0239
Logarithmic	$a = 0.735 \ k = 0.208 \ c = 0.277$	0.996	0.0120	$a = 0.596 \ k = 0.192 \ c = 0.404$	0.997	0.0069
Two term	$a = 0.031 \ b = 0.976$ $k_0 = -0.168 \ k_1 = 0.15$	0.998	0.0069	$a = 0.87 \ b = 0.126 \ k_0 = 0.133$ $k_1 = -0.075$	0.998	0.0069
Wang and Singh	$a = -0.127 \ b = 0.007$	0.998	0.0069	$a = -0.099 \ b = 0.005$	0.997	0.0098
Modified Page	$k = 0.108 \ n = 0.834$	0.989	0.0195	$k = 0.071 \ n = 0.773$	0.986	0.0183
Thompson	$a = -5.36 \ b = 4.412$	0.985	0.3727	$a = -6.424 \ b = 10.215$	0.992	0.2661



(a) OSD



(b) hybrid solar dryer

Figure 10. The relationship between predicted and experimental values for lemon slices' drying.

4.2. Energy and Exergy Analysis

The set of experiments data for studying the operation performance of hybrid solar dryer were carried out on 1–3 June 2018. The change of solar radiation intensity and ambient temperature are shown in Figure 11. The red dotted line indicates the end of the previous dry day and the beginning of the next dry day. In the process of drying lemon slices, the solar radiation intensity ranged from 33 W/m^2 to 618 W/m^2 . The variation amplitude of solar radiation intensity was relatively large on the first drying day. In addition, the maximum of solar radiation intensity occurred at the time of 11:30~14:00. The ambient temperature varied from $25.6 \text{ }^\circ\text{C}$ to $37.5 \text{ }^\circ\text{C}$ with an average of $32.08 \text{ }^\circ\text{C}$.

Figure 12 represents the change of different parts temperature and relative humidity. The inlet and outlet air temperature range of drying cabinet were from $27.6 \text{ }^\circ\text{C}$ to $52.8 \text{ }^\circ\text{C}$ and from $27.8 \text{ }^\circ\text{C}$ to $54 \text{ }^\circ\text{C}$, respectively. The relative humidity of ambient air and the drying chamber inside varied from 31.3% to 59.2% and 10.7% to 34.9%, respectively. The average inlet and outlet air temperature of the drying chamber were $43.39 \text{ }^\circ\text{C}$ and $43.14 \text{ }^\circ\text{C}$, respectively. See Figure 12, the outlet air temperature of drying chamber was occasionally higher than the inlet air temperature of the drying chamber, it was not consistent with the research results of Rabha et al. [22], this is because the drying chamber type in this study is different from Rabha et al. [22]. The experimental results of this study were similar to those of Elkhadraoui et al. [10]. Furthermore, the average relative humidity of ambient air and drying chamber inside were 45.14% and 17.36%, respectively.

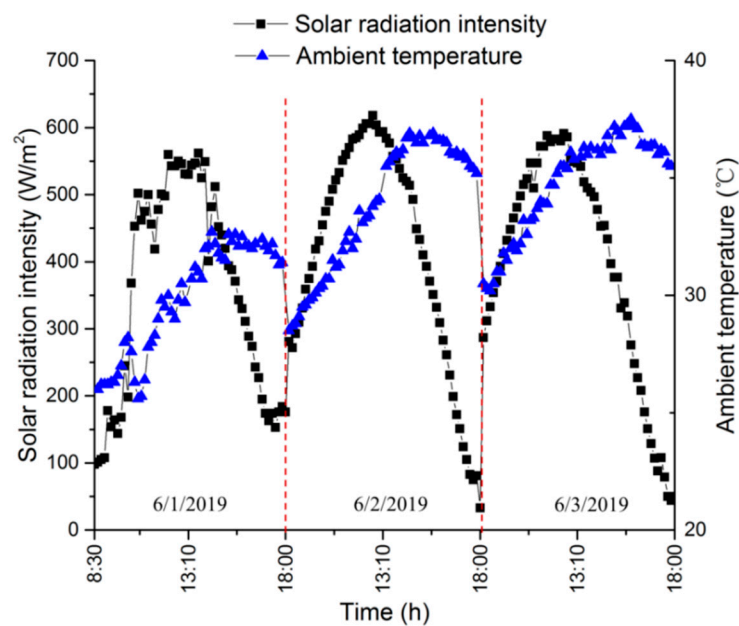


Figure 11. The change of solar radiation intensity and ambient temperature.

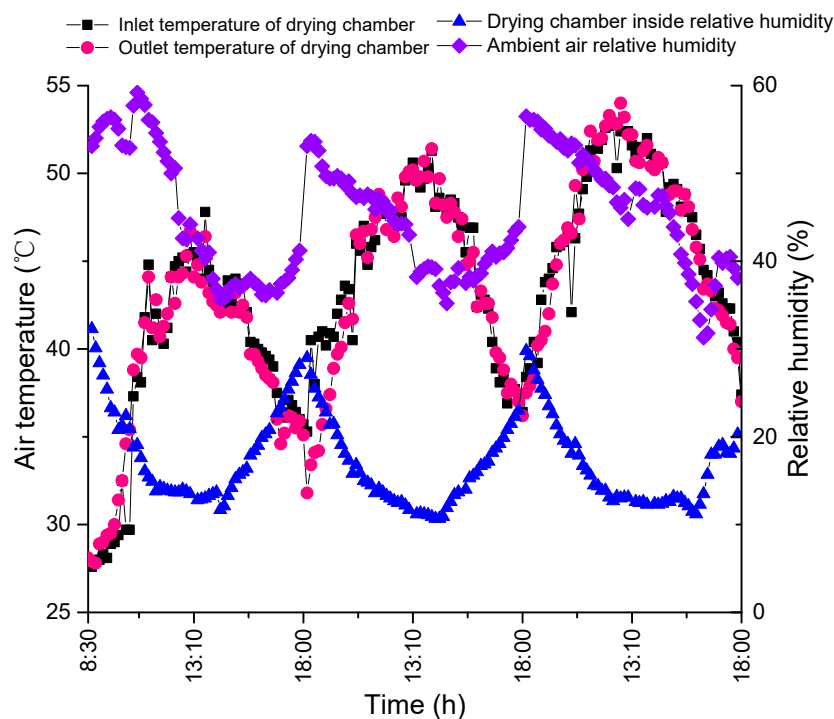


Figure 12. The variation of different parts' temperature and relative humidity.

Figure 13 shows the change of lemon slice moisture content. The moisture content of lemon slices was reduced from initial moisture content (w.b) of 83.6 g g^{-1} to 10.3 g g^{-1} during the drying time of 27 h. The change trend of drying lemon slices was similar to that of other drying products such as red pepper [47], thymus and mint [21], and rubber sheet [18].

Figure 14 represents the change of drying chamber air temperature and thermal efficiency. The air temperature of the drying chamber varied from $29.2 \text{ }^{\circ}\text{C}$ to $60.4 \text{ }^{\circ}\text{C}$ with an average of $48.97 \text{ }^{\circ}\text{C}$. The maximum air temperature of the drying chamber can be controlled under $60 \text{ }^{\circ}\text{C}$. It was shown that the operation of the system can effectively avoid the influence of high temperature on the quality of dry

products. Dimitrios and Joachim [48] demonstrated that excessive drying temperature can result in deteriorating the drying product's color. Meanwhile, the thermal efficiency of collector was in range of 2% to 69.52% with an average of 44.6%.

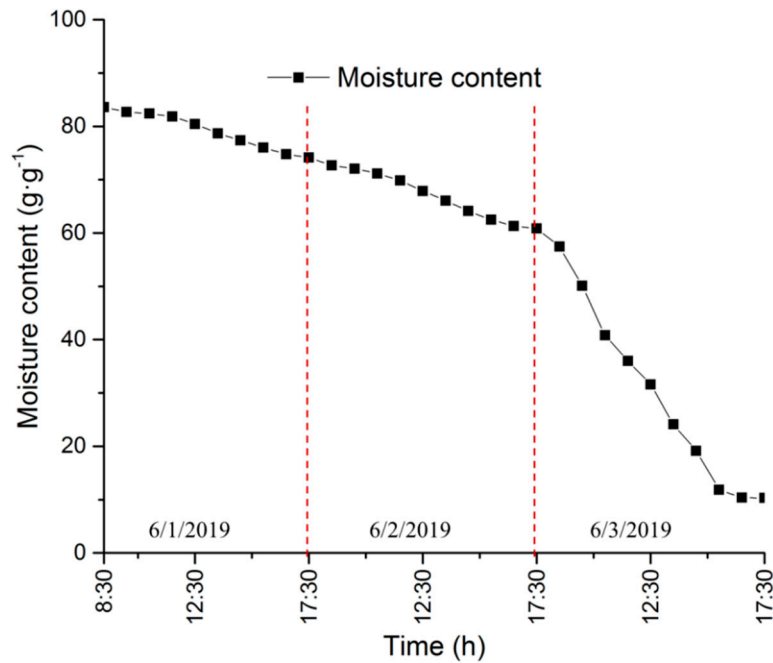


Figure 13. The variation of lemon slice moisture content.

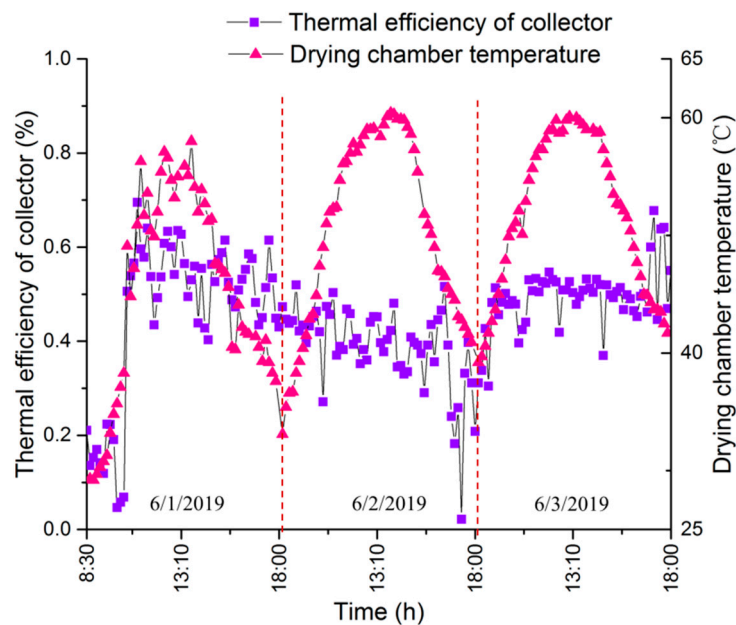


Figure 14. The change of drying chamber air temperature and thermal efficiency.

Figure 15 exhibits the variation of exergy flow, loss and efficiency. The exergy flow of the drying cabinet inlet and outlet ranged from 6.46 W to 359.34 W and 0.68 W to 149.42 W, respectively, and the change trend of exergy inflow and outflow was to increase first and then decrease. The maximum value of exergy inflow and outflow occurred at 11:10, 11:20, respectively. Furthermore, the exergy loss and efficiency varied from 3.42 W to 239.35 W and 39.38% to 71.7%, respectively, in the drying cabinet. The maximum exergy efficiency appeared in the end of each drying day. Boulemtafes-Boukadoum

et al. [49], Sami et al. [50] and Kesavan et al. [51] found a similar research result for drying chamber exergy analysis.

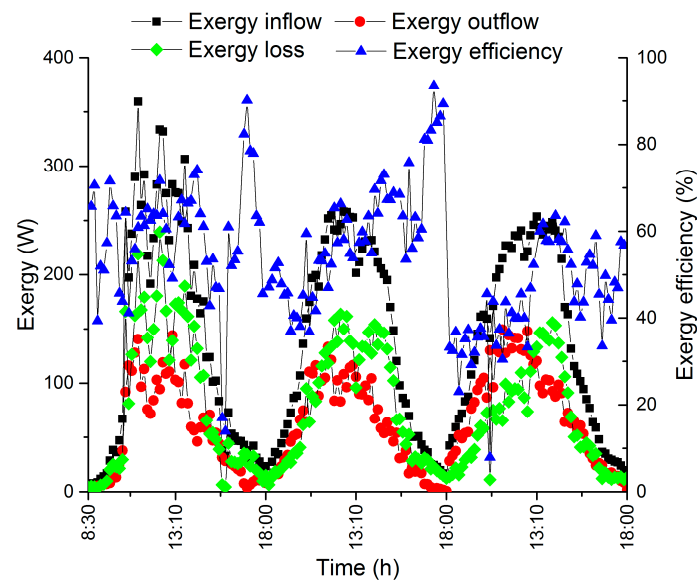


Figure 15. The variation of exergy flow, loss and efficiency.

Figure 16 represents the variation of improvement potential (IP) and theoretical thermal efficiency of the drying cabinet. The improvement potential range of drying cabinet was from 0.65 W to 85.56 W. The change trend of improvement potential is to increase first and then decrease at each drying day. This result was similar to that of Fudholi et al. [23]. The theoretical thermal efficiency of the drying chamber varied from 4.5% to 78% with an average of 36.47%. It can be concluded that the drying chamber can be improved by adding insulation measures [22,52]. The performance parameters for drying lemon slices are summarized in Table 6. The specific energy consumption of hybrid solar dryer is 4.05 kW·h/kg, which was lower than that of Fudholi et al. [53] (5.26 kW·h/kg for red chili), Rabha et al. [22] (18.72 kW·h/kg for ghost chilli pepper and 8.82 kW·h/kg for ginger) and was higher than that of Fudholi et al. [23] (2.62 kW·h/kg for red seaweed). It can be concluded that the specific energy consumption of a drying system is different based on different drying products.

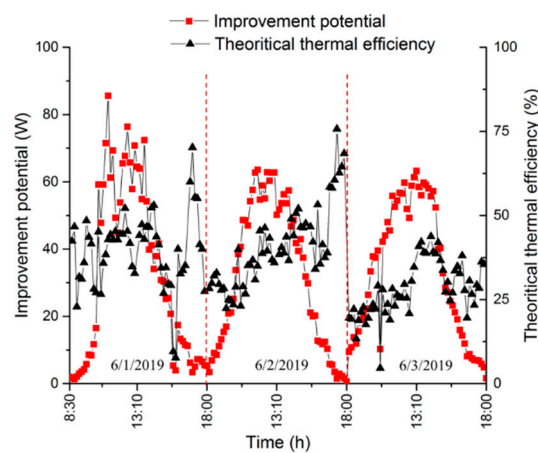


Figure 16. The variation of improvement potential and theoretical thermal efficiency.

Table 6. Performance parameters of hybrid solar dryer for drying lemon slices.

Performance Parameters	Value	Unit
Initial mass (lemon slices)	4.12	kg
Final mass (lemon slices)	0.55	kg
Total drying time	27	h
Specific energy consumption	4.05	kW·h/kg
Initial moisture content (w.b)	83.6	%
Electrical consumption of fan	2.28	kW·h
Electrical consumption of pump	0.75	kW·h
Final moisture content (w.b)	10.3	%
Thermal efficiency of collector	2~69.52	%
Thermal efficiency of hybrid solar dryer	9.5	%
Exergy inflow of hybrid solar dryer	6.46~359.34	W
Exergy outflow of hybrid solar dryer	0.68~149.42	W
Exergy efficiency of hybrid solar dryer	39.38~71.7	%

4.3. Economic and Environment Analysis

The set of experiments data for analyzing economic and environment of hybrid solar dryer were carried out on 1–3 June 2018. The economic analyses were carried out based on the current hybrid solar dryer and china economic situation. The economic analysis results of the hybrid solar dryer are listed in Table 7. The capital cost of the hybrid solar dryer is 5700 RMB. The drying capacity of the hybrid solar dryer is 5 kg for lemon slices. The hybrid solar dryer can be used for 4 months according to the local climate parameters. It can be concluded that the payback period was 3.63 years compared to the lifetime of the hybrid solar dryer (5 years).

Table 7. The economic analysis results of the hybrid solar dryer.

Parameters	Value	Unit
Material cost (collector, fan, pipe etc.)	3500	RMB
Construction cost	2200	RMB
Maintenance cost	57	RMB
Electricity price	0.8	RMB/kW·h
Fresh lemon price	22.9	RMB/kg
Dried lemon price	169	RMB/kg
Lifetime	5	Year
Interest rate	5.63	%
Inflation rate	2.5	%
Pay-back period	3.63	Year
Annual cost calculation	1177	RMB
Cost per unit of drying materials	5.89	RMB/kg

The environmental analyses of the hybrid solar dryer were conducted based on a batch of dried lemon products. By using Equation (36), the CO₂ reduction per batch based on results of this experiment was 21.79 kg/batch. The revenue of CO₂ abatement per batch was 1.61 RMB/batch by using Equations (37) and (38). The results show that the system has good economic and environmental benefits.

4.4. Analysis of Hybrid Solar Dryer Operation Mode

The set of experimental data for studying hybrid solar dryer operation mode was gathered on 7 and 8 June 2018. Due to the fact that high drying temperature will affect the quality of the drying sample [54], the working principle of hybrid solar dryer operation mode is to control the air temperature inside chamber at less than 60 °C. According to Figure 6, the maximum drying air temperature is 60.2 °C in the cabinet, which meets the demand of the hybrid solar dryer operation working principle. The variation of DF-FPSC air and water outlet temperature is shown in Figure 17. It can be found

that the air temperature of the collector outlet decreases instantly while the water temperature rises. The start-up time of the water pump was 12:51, 12:19, respectively, for two days. This was because the dry cabinet air temperature was higher than the suitable product drying temperature. There are two operation modes (only air cycle and air and water simultaneous cycle) in the process of DF-FPSC operation. According to Equations (18) and (19), the average solar collector efficiency under different operation mode was 42.9% (only air), 47.4% (air and water simultaneous cycle) with the air flow rate of 28.125 m³/h and the water flow rate of 1.125 m³/h on the first day; the average solar collector efficiency under different operation mode was 39.2% (only air), 41.4% (air and water simultaneous cycle) with the air flow rate of 28.125 m³/h and water flow rate of 1.125 m³/h on the second day. Based on the analysis of the above experimental results, the experimental results show the feasibility and validity of the proposed hybrid solar dryer.

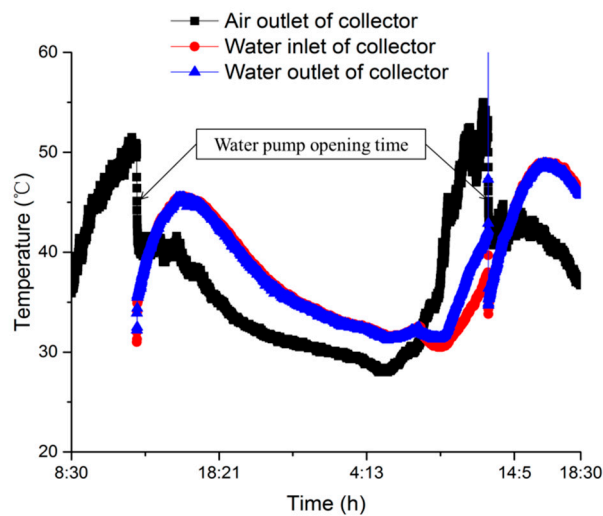


Figure 17. The variation of DF-FPSC air and water outlet temperature.

5. Conclusions

A new hybrid solar dryer with DF-FPSC was designed and constructed in this study; and drying experiments for lemon slices (initial moisture content 82.8% on a wet basis) were carried out under hybrid solar dryer and OSD conditions. The drying characteristics and operational performance of the hybrid solar dryer for drying lemon slices have been analyzed. From the above studies, the following conclusions have been reached:

- Under the same drying time condition, the drying capacity of the hybrid solar dryer is better than OSD. Meanwhile, it was found that the Two term model and Wang and Singh model were the best suitable models to describe the lemon slices drying characteristics for hybrid solar dryer. The Two term model was only the best model for OSD.
- The efficiency range of DF-FPSC was from 2% to 69.52% with an average of 44.6%. The exergy flow of the drying cabinet inlet and outlet ranged from 6.46 W to 359.34 W and 0.68 W to 149.42 W, respectively. The exergy efficiency range of the drying cabinet was from 39.38% to 71.7%, respectively. The improvement potential range of the drying cabinet was from 0.65 W to 85.56 W. It can be concluded that the outlet of the drying chamber lost considerable energy.
- It was found that the pay-back period was 3.63 years. The CO₂ reduction per batch based on the results of this experiment was 21.79 kg/batch. The revenue of CO₂ abatement per batch was 1.61 RMB/batch. The system has good economic and environmental benefits.
- During the period of hybrid solar dryer operation, the maximum drying air temperature can be controlled under 60.2 °C in the cabinet. The start-up time of the water pump was 12:51, 12:19, respectively, for two days. This was because the dry cabinet air temperature was higher than the

suitable product drying temperature. The experimental results showed the feasibility and validity of the proposed hybrid solar dryer with DF-FPSC.

Author Contributions: W.H. developed systematic idea and wrote manuscript; S.L. and B.M. did experimental test; Y.L. reviewed the manuscript. All authors have read and agreed to the published version of the manuscript.

Funding: This research was funded by the National Natural Science Foundation of China (Grant No. 51476093).

Conflicts of Interest: The authors declare no conflict of interest.

Nomenclature

Nomenclature

W_d	Final mass of products (g)
$M_{d,0}$	Initial moisture content on dry basis (g g^{-1})
w	Uncertainty
IP	Improvement potential (W)
M	Moisture content (g g^{-1})
i	Year
W_t	Evaporate quantity of water at t time (g)
M_e	Equilibrium moisture content (g g^{-1})
MR	Moisture ratio
R^2	Regression coefficient
Ex	Exergy (W)
SEC	Specify energy consumption ($\text{kW}\cdot\text{h}/\text{kg}$)
DR	Drying rate of products ($\text{g g}^{-1} \text{ s}^{-1}$)
C_t	Capital cost (RMB)
RMSE	Root mean square error
a, b, k, n, k_0, k_1	Constant used in models
m	Mass flow (m^3/h)
Q_u	Useful energy (J)
$I(t)$	Solar radiation intensity (W/m^2)
A_c	Collector area (m^2)
$M_{w,0}$	Initial moisture content on wet basis (g g^{-1})
C_m	Material cost (RMB)
C_c	Construction cost (RMB)
C_a	Annual cost (RMB)
t	Time (s)
PBP	Payback period (year)
P	Cost per unit of drying materials (RMB/kg)
R	CO_2 reductions (kg CO_2)
EM	CO_2 emission (kg CO_2)
CP	International carbon price (RMB/ton)
Y	Renue of CO_2 abatement (RMB)
C_p	Specific heat capacity ($\text{kJ}/(\text{kg } ^\circ\text{C})$)
T	Temperature ($^\circ\text{C}$)
<i>Greek symbols</i>	
δ	Saving-time percentage of drying
ψ_{CO_2}	Average CO_2 equivalent intensity for electricity generation from coal ($\text{kg CO}_2/\text{kW}\cdot\text{h}$)
α	Absorptivity
τ	Transmissivity
ϕ	Relative humidity (%)
η	Thermal efficiency of collector

Subscripts and abbreviations

0	Initial time
<i>a</i>	Air
mp	Moisture of product
<i>exp</i>	Experimental
<i>pre</i>	Predicted
<i>sat</i>	Saturated
<i>w</i>	Water
<i>i</i>	Number
<i>ou</i>	Outlet
<i>in</i>	Inlet
<i>ev</i>	Evaporate
<i>th</i>	Theoretical thermal efficiency
<i>dc</i>	Drying chamber
<i>ref</i>	Reference value
<i>c</i>	Collector
<i>f</i>	Final time

References

1. Pirasteh, G.; Saidur, R.; Rahman, S.M.A.; Rahim, N.A. A review on development of solar drying applications. *Renew. Sustain. Energy Rev.* **2014**, *31*, 133–148. [[CrossRef](#)]
2. Fudholi, A.; Sopian, K.; Bakhtyar, B.; Gabbasa, M.; Othman, M.Y.; Ruslan, M.H. Review of solar drying systems with air based solar collectors in Malaysia. *Renew. Sustain. Energy Rev.* **2015**, *51*, 1191–1204. [[CrossRef](#)]
3. Mustayen, A.G.M.B.; Mekhilef, S.; Saidur, R. Performance study of different solar dryers: A review. *Renew. Sustain. Energy Rev.* **2014**, *34*, 463–470. [[CrossRef](#)]
4. Goh, L.J.; Othman, M.Y.; Mat, S.; Ruslan, H.; Sopian, K. Review of heat pump systems for drying application. *Renew. Sustain. Energy Rev.* **2011**, *15*, 4788–4796. [[CrossRef](#)]
5. Fadhel, M.I.; Sopian, K.; Daud, W.R.W.; Alghoul, M.A. Review on advanced of solar assisted chemical heat pump dryer for agriculture produce. *Renew. Sustain. Energy Rev.* **2011**, *15*, 1152–1168. [[CrossRef](#)]
6. El-Sebaei, A.A.; Shalaby, S.M. Solar drying of agricultural products: A review. *Renew. Sustain. Energy Rev.* **2012**, *16*, 37–43. [[CrossRef](#)]
7. Kumar, M.; Sansaniwal, S.K.; Khatak, P. Progress in solar dryers for drying various commodities. *Renew. Sustain. Energy Rev.* **2016**, *55*, 346–360. [[CrossRef](#)]
8. Banout, J.; Ehl, P.; Havlik, J.; Lojka, B.; Polesny, Z.; Verner, V. Design and performance evaluation of a Double-pass solar drier for drying of red chilli (*Capsicum annum* L.). *Sol. Energy* **2011**, *85*, 506–515. [[CrossRef](#)]
9. Tiwari, S.; Tiwari, G.N.; Al-Helal, I.M. Performance analysis of photovoltaic-thermal (PVT) mixed mode greenhouse solar dryer. *Sol. Energy* **2016**, *133*, 421–428. [[CrossRef](#)]
10. Elkhadraoui, A.; Kooli, S.; Hamdi, I.; Farhat, A. Experimental investigation and economic evaluation of a new mixed-mode solar greenhouse dryer for drying of red pepper and grape. *Renew. Energy* **2015**, *77*, 1–8. [[CrossRef](#)]
11. Kabeel, A.E.; Abdelgaied, M. Performance of novel solar dryer. *Process Saf. Environ.* **2016**, *102*, 183–189. [[CrossRef](#)]
12. Janjai, S.; Lamlert, N.; Intawee, P.; Mahayothee, B.; Bala, B.K.; Nagle, M.; Müller, J. Experimental and simulated performance of a PV-ventilated solar greenhouse dryer for drying of peeled longan and banana. *Sol. Energy* **2009**, *83*, 1550–1565. [[CrossRef](#)]
13. Aktaş, M.; Şevik, S.; Amini, A.; Khanlari, A. Analysis of drying of melon in a solar-heat recovery assisted infrared dryer. *Sol. Energy* **2016**, *137*, 500–515. [[CrossRef](#)]
14. Sonthikun, S.; Chairat, P.; Fardsin, K.; Kirirat, P.; Kumar, A.; Tekasakul, P. Computational fluid dynamic analysis of innovative design of solar-biomass hybrid dryer: An experimental validation. *Renew. Energy* **2016**, *92*, 185–191. [[CrossRef](#)]
15. Can, A. Drying kinetics of pumpkinseeds. *Int. J. Energy Res.* **2000**, *24*, 965–975. [[CrossRef](#)]

16. Gulcimen, F.; Karakaya, H.; Durmus, A. Drying of sweet basil with solar air collectors. *Renew. Energy* **2016**, *93*, 77–86. [[CrossRef](#)]
17. Ali, I.; Abdelkader, L.; El Houssayne, B.; Mohamed, K.; El Khadir, L. Solar convective drying in thin layers and modeling of municipal waste at three temperatures. *Appl. Therm. Eng.* **2016**, *108*, 41–47. [[CrossRef](#)]
18. Dejchanchaiwong, R.; Arkasuwan, A.; Kumar, A.; Tekasakul, P. Mathematical modeling and performance investigation of mixed-mode and indirect solar dryers for natural rubber sheet drying. *Energy Sustain. Dev.* **2016**, *34*, 44–53. [[CrossRef](#)]
19. Kooli, S.; Fadhel, A.; Farhat, A.; Belghith, A. Drying of red pepper in open sun and greenhouse conditions. Mathematical modeling and experimental validation. *J. Food Eng.* **2007**, *79*, 1094–1103. [[CrossRef](#)]
20. Bennamoun, L.; Belhamri, A. Numerical simulation of drying under variable external conditions: Application to solar drying of seedless grapes. *J. Food Eng.* **2006**, *76*, 179–187. [[CrossRef](#)]
21. El-Sebaai, A.A.; Shalaby, S.M. Experimental investigation of an indirect-mode forced convection solar dryer for drying thymus and mint. *Energy Convers. Manag.* **2013**, *74*, 109–116. [[CrossRef](#)]
22. Rabha, D.K.; Muthukumar, P.; Somayaji, C. Energy and exergy analyses of the solar drying processes of ghost chilli pepper and ginger. *Renew. Energy* **2017**, *105*, 764–773. [[CrossRef](#)]
23. Fudholi, A.; Sopian, K.; Othman, M.Y.; Ruslan, M.H. Energy and exergy analyses of solar drying system of red seaweed. *Energy Build.* **2014**, *68*, 121–129. [[CrossRef](#)]
24. Akbulut, A.; Durmuş, A. Energy and exergy analyses of thin layer drying of mulberry in a forced solar dryer. *Energy* **2010**, *35*, 1754–1763. [[CrossRef](#)]
25. Midilli, A.; Kucuk, H. Energy and exergy analyses of solar drying process of pistachio. *Energy* **2003**, *28*, 539–556. [[CrossRef](#)]
26. Nayak, S.; Tiwari, G.N. Energy and exergy analysis of photovoltaic/thermal integrated with a solar greenhouse. *Energy Build.* **2008**, *40*, 2015–2021. [[CrossRef](#)]
27. Sarhaddi, F.; Farahat, S.; Ajam, H.; Behzadmehr, A. Exergetic performance assessment of a solar photovoltaic thermal (PV/T) air collector. *Energy Build.* **2010**, *42*, 2184–2199. [[CrossRef](#)]
28. Prakash, O.; Kumar, A. Environomical analysis and mathematical modelling for tomato flakes drying in a modified greenhouse dryer under active mode. *Int. J. Food Eng.* **2014**, *10*, 669–681. [[CrossRef](#)]
29. Chen, H.H.; Hernandez, C.E.; Huang, T.C. A study of the drying effect on lemon slices using a closed-type solar dryer. *Sol. Energy* **2005**, *78*, 97–103. [[CrossRef](#)]
30. Wang, J.; Law, C.L.; Nema, P.K.; Zhao, J.H.; Liu, Z.L.; Deng, L.Z.; Gao, Z.J.; Xiao, H.W. Pulsed vacuum drying enhances drying kinetics and quality of lemon slices. *J. Food Eng.* **2018**, *224*, 129–138. [[CrossRef](#)]
31. Fudholi, A.; Sopian, K.; Ruslan, M.H.; Alghoul, M.A.; Sulaiman, M.Y. Review of solar dryers for agricultural and marine products. *Renew. Sustain. Energy Rev.* **2010**, *14*, 1–30. [[CrossRef](#)]
32. Hao, W.; Lu, Y.; Lai, Y.; Yu, H.; Lyu, M. Research on operation strategy and performance prediction of flat plate solar collector with dual-function for drying agricultural products. *Renew. Energy* **2018**, *127*, 685–696. [[CrossRef](#)]
33. El-Sebaai, A.A.; Aboul-Enein, S.; Ramadan, M.R.I.; El-Gohary, H.G. Empirical correlations for drying kinetics of some fruits and vegetables. *Energy* **2002**, *27*, 845–859. [[CrossRef](#)]
34. Jayas, D.S.; Cenkowski, S.; Pabis, S.; Muir, W.E. Review of thin-layer drying and wetting equations. *Dry Technol.* **1991**, *9*, 551–588. [[CrossRef](#)]
35. Page, G.E. Factors Influencing the Maximum Rates of Air Drying Shelled Corn in Thin Layers. Master's Thesis, Purdue University, Purdue, IN, USA, 1949.
36. Henderson, S.M.; Pabis, S. Grain drying theory. *J. Agric. Eng. Res.* **1961**, *6*, 169–174.
37. Yagcioglu, A.; Degirmencioglu, A.; Cagatay, F. Drying characteristic of laurel leaves under different conditions. In Proceedings of the 7th International Congress on Agricultural Mechanization and Energy, Adana, Turkey, 26–27 May 1999; pp. 565–569.
38. Henderson, S.M. Progress in developing the thin layer drying equation. *Trans. ASAE* **1974**, *17*, 1167–1168. [[CrossRef](#)]
39. Wang, C.Y.; Singh, R.P. *A Single Layer Drying Equation for Rough Rice*; ASAE: St. Joseph, MI, USA, 1978; pp. 78–3001.
40. White, G.M.; Bridges, T.C.; Loewer, O.J.; Ross, I.J. *Seed Coat Damage in Thin Layer Drying of Soybeans as Affected by Drying Conditions*; ASAE: St. Joseph, MI, USA, 1978; p. 3052.

41. Thompson, T.L. Predicted Performances and Optimal Designs of Convection Grain Dryers. Ph.D. Thesis, Purdue University, Lafayette, IN, USA, 1967.
42. Audsley, E.W.J. The annual cost of machinery calculated using actual cash flows. *J. Agric. Eng. Res.* **1978**, *23*, 189–201. [[CrossRef](#)]
43. Tripathi, R.; Tiwari, G.N.; Dwivedi, V.K. Overall energy, exergy and carbon credit analysis of N partially covered Photovoltaic Thermal (PVT) concentrating collector connected in series. *Sol. Energy* **2016**, *136*, 260–267. [[CrossRef](#)]
44. Mghazli, S.; Ouhammou, M.; Hidar, N.; Lahnine, L.; Idlimam, A.; Mahrouz, M. Drying characteristics and kinetics solar drying of Moroccan rosemary leaves. *Renew. Energy* **2017**, *108*, 303–310. [[CrossRef](#)]
45. De Lima, A.G.B.; Queiroz, M.R.; Nebra, S.A. Simultaneous moisture transport and shrinkage during drying of solids with ellipsoidal configuration. *Chem. Eng. J.* **2002**, *86*, 85–93. [[CrossRef](#)]
46. Kaewkiew, J.; Nabnean, S.; Janjai, S. Experimental investigation of the performance of a large-scale greenhouse type solar dryer for drying chilli in Thailand. *Procedia Eng.* **2012**, *32*, 433–439. [[CrossRef](#)]
47. Hamdi, I.; Elkhadraoui, A.; Kooli, S.; Farhat, A.; Guizani, A. Drying of red pepper slices in a solar greenhouse dryer and under open sun: Experimental and mathematical investigations. *Innov. Food Sci. Emerg.* **2019**, *52*, 262–270.
48. Argyropoulos, D.; Müllera, J. Effect of Convective Drying on Quality of Lemon Balm (*Melissa officinalis* L.). *Procedia Food Sci.* **2011**, *1*, 1932–1939. [[CrossRef](#)]
49. Boulemtafes-Boukadoum, A.; Benzaoui, A. Energy and exergy analysis of solar drying process of Mint. *Energy Procedia* **2011**, *6*, 583–591. [[CrossRef](#)]
50. Sami, S.; Etesami, N.; Rahimi, A. Energy and exergy analysis of an indirect solar cabinet dryer based on mathematical modeling results. *Energy* **2011**, *36*, 2847–2855. [[CrossRef](#)]
51. Kesavan, S.; Arjunan, T.V.; Vijayan, S. Thermodynamic analysis of a triple-pass solar dryer for drying potato slices. *J. Therm. Anal. Calorim.* **2018**, *136*, 159–171. [[CrossRef](#)]
52. Akpınar, E.K. Drying of mint leaves in a solar dryer and under open sun: Modelling, performance analyses. *Energy Convers. Manag.* **2010**, *51*, 2407–2418. [[CrossRef](#)]
53. Fudholi, A.; Sopian, K.; Yazdi, M.H.; Ruslan, M.H.; Gabbasa, M.; Kazem, H.A. Performance analysis of solar drying system for red chili. *Sol. Energy* **2014**, *99*, 47–54. [[CrossRef](#)]
54. Vega, A.; Fito, P.; Andrés, A.; Lemus, R. Mathematical modeling of hot-air drying kinetics of red bell pepper. *J. Food Eng.* **2007**, *79*, 1460–1466. [[CrossRef](#)]



© 2020 by the authors. Licensee MDPI, Basel, Switzerland. This article is an open access article distributed under the terms and conditions of the Creative Commons Attribution (CC BY) license (<http://creativecommons.org/licenses/by/4.0/>).